



## Abstract

The longest six instrumental temperature records of monthly means reach back maximally to 1757 AD and were recorded in Europe. All six show a V-shape, with temperature drop in the 19th and rise in the 20th century. Proxy temperature time series of Antarctic ice cores show this same characteristic shape, indicating this pattern as a global phenomenon. We used the mean of the 6 instrumental records for analysis by discrete Fourier transformation (DFT), wavelets, and the detrended fluctuation method (DFA). For comparison, a stalagmite record was also analyzed by DFT. The harmonic decomposition of the mean shows only 6 significant frequencies above periods over 30 yr. The Pearson correlation between the mean, smoothed by a 15 yr running average (boxcar) and the reconstruction using the 6 significant frequencies yields  $r = 0.961$ . This good agreement has a  $> 99.9\%$  confidence level confirmed by Monte Carlo simulations. Assumption of additional forcing by anthropogenic green house gases would therefore not improve the agreement between measurement and temperature construction from the 6 documented periodicities. We find indications that the observed periodicities result from intrinsic system dynamics.

## 1 Introduction

It is widely accepted that the mean surface temperature of the globe has been rising in the 20th century. However, how strong and how unusual this rise in comparison with the temperature variations over the last 250 or even 2000 yr was is one of the subjects in the actual climate debate. Long-range instrumental records going back to a maximum of about 250 yr BP exist only in Central Europe. But even here they are not abundant. The places with reliable monthly time series number six in all: Prague, Hohenpeisenberg, Kremsmünster, Vienna, Paris and Munich (CRU, 2012; DWD, 2012; Auer et al., 2007; Météo France, 2012; CHMI, 2012). They have some of the longest, most reliable instrumental temperature records as monthly means to be had anywhere. The

CPD

8, 4493–4511, 2012

## Multi-periodic climate dynamics

H.-J. Lüdecke et al.

Title Page

Abstract

Introduction

Conclusions

References

Tables

Figures

⏪

⏩

◀

▶

Back

Close

Full Screen / Esc

Printer-friendly Version

Interactive Discussion



time series of Paris begins in 1757 AD whereas those of Hohenpeissenberg and Munich begin only in 1781 AD. Additionally, a high quality temperature proxy record from a stalagmite retrieved in the Spannagel Cave near Innsbruck (Austria) at 2347 m.a.s.l. is available ranging from 90 BC until 1935 AD (Mangini et al., 2005). It has time steps between 1 yr and 13 yr. Finally, a yearly  $\delta^{18}\text{O}$  record of the period 1801–1997 AD from the analysis of an Antarctic ice core is available for further comparison (Graf et al., 2002).

We used the temperature anomalies divided by the standard deviations for each of the above cited 6 instrumental records from Central Europe. As these are rather close to one another, we used the mean of these (hereafter M6) for the numerical analysis. Equally the anomalies of the stalagmite record and the ice core record, divided by the standard deviations were analyzed (hereafter SPA for the stalagmite record and IC for the ice core record).

Figure 1 depicts the 6 normalized time series whose average is M6. They all show a typical V-pattern with a maximum around the year 1800 AD, a fall until a minimum at about 1880 AD, and a rise until the recent maximum at about 2000 AD. Both maxima have similar magnitudes. Figure 2 gives M6 superimposed with IC showing the V-shape of the temperature history equally in the Northern and Southern Hemisphere, and therefore as a global phenomenon.

The time series M6 and SPA are analyzed by the discrete Fourier transform (DFT) with zero padding. Zero padding in the time domain increases the frequency steps and corresponds to an ideal interpolation in the frequency domain. To obtain information about the significance of the peaks, we adjoin in the DFT spectra the 90% and the 95% confidence limits of the background noise evaluated by Monte Carlo simulations. Next, an empirical reconstruction of M6 based on the results of a DFT without zero padding is executed which is restricted to oscillations of periods not shorter than 30 yr. Due to the quality of the reconstruction, conclusions about the climate for the coming decades can be drawn.

**Multi-periodic  
climate dynamics**

H.-J. Lüdecke et al.

Title Page

Abstract

Introduction

Conclusions

References

Tables

Figures

◀

▶

◀

▶

Back

Close

Full Screen / Esc

Printer-friendly Version

Interactive Discussion



## 2 The data basis

The instrumental records from Central Europe consist of monthly means and are continuous except for Paris and Munich which are made up each of two parts from different nearby stations. However, both for Paris and Munich the major part of the two single time series covers nearly the whole record length. The monthly means are converted to yearly means for the application of the DFT. In contrast to this, both the stalagmite record SPA and the ice core record IC consist of yearly means. The details of the records used in this paper are: Kremsmünster, monthly (1768–2010) (Auer et al., 2007); Hohenpeissenberg, monthly (1781–2010) (CRU, 2012); Prague, monthly (1770–2010) (CHMI, 2012); Paris-Le-Bourget, monthly (1757–1993) (Météo France, 2012), Paris-Montsouris, monthly (1994–2011) (Météo France, 2012); Munich-Riem, monthly (1781–2007) (Auer et al., 2007), Munich-Airport, monthly (2007–2011) (DWD, 2012); Vienna, monthly (1775–2010) (CRU, 2012); Stalagmite record SPA, unequally yearly (–90–1935) (Mangini et al., 2005); Ice core record IC, yearly (1801–1997) (Graf et al., 2002).

## 3 Methods

In the literature, several methods for the spectral analysis of time series are reported (Ghil et al., 2002). We used in this study the simple method of the discrete Fourier transformation (DFT). The time series M6 has equal time steps of one year and, therefore, the DFT can be applied without any further complications. However, for SPA which has unequal time steps the DFT requires an interpolation procedure in the time domain. With the data  $f_k$  in the time domain and  $N$  as the number of  $f_k$  (here  $N = 254$ ) the DFT is

$$F_j = \frac{1}{N} \sum_{k=0}^{N-1} f_k W_N^{-kj} \quad (1)$$

Title Page

Abstract

Introduction

Conclusions

References

Tables

Figures

◀

▶

◀

▶

Back

Close

Full Screen / Esc

Printer-friendly Version

Interactive Discussion



with  $W_N = e^{2\pi i/N}$  and the reverse transformation

$$f_k = \sum_{j=0}^{N-1} F_j W_N^{kj} \quad (2)$$

In principle, for unequally spaced time steps the DFT is not applicable. Interpolation in the time domain, however, can result in enhancing the low frequencies and reducing the high frequency components (Schulz and Mudelsee, 2002). Therefore, we compared in a first step the result of the interpolated SPA record yielded by DFT with the result of the unmodified SPA record yielded by the periodogram method (Horne and Baliunas, 1986). As an outcome, no significant differences in the peak frequencies but differences in the peak strengths occur between DFT with the interpolated SPA and the periodogram with the unchanged SPA. Because the stalagmite record SPA is predominantly used in this paper for a comparison of frequencies with M6 and because the widest time steps of SPA lie in the period from 90 BC until 500 AD, we omitted the first years of 90 BC until 500 AD and carried out again the comparison of the DFT with the periodogram. As a result, we find for the shortened interpolated SPA both for the frequencies and the power densities good accordance of the DFT and the periodogram. To obtain more frequency steps we generally applied zero padding in the DFT except for the empirical reconstruction of M6. Furthermore, the power values  $F_j$  in Eq. (1) were normalized by the area below them.

In order to obtain confidence levels of the background noise, the autocorrelation (persistence) of the records M6 and SPA has to be considered. The appropriate method for the evaluation of the persistence of a time series is the detrended fluctuation analysis (DFA) specified in (Kantelhardt, 2004), (Lennartz and Bunde, 2009, 2011) and references cited therein. In general, one visualizes the significance of peaks in DFT power spectra against the background noise with lines of 90 %, 95 % or 99 % confidence levels and assumes a background of red noise as an AR1 process (Schulz and Mudelsee, 2002). We applied a more realistic procedure that accounts for the autocorrelation of

## Multi-periodic climate dynamics

H.-J. Lüdecke et al.

Title Page

Abstract

Introduction

Conclusions

References

Tables

Figures



Back

Close

Full Screen / Esc

Printer-friendly Version

Interactive Discussion



**Multi-periodic  
climate dynamics**

H.-J. Lüdecke et al.

Title Page

Abstract

Introduction

Conclusions

References

Tables

Figures

◀

▶

◀

▶

Back

Close

Full Screen / Esc

Printer-friendly Version

Interactive Discussion



the record: The autocorrelation (persistence) of a time series is characterized by its Hurst exponent  $\alpha$  which can be evaluated with DFA. For the stalagmite record SPA an  $\alpha$  of 0.9 was already reported (Lüdecke, 2011), which indeed corresponds roughly to a red noise background. However, our DFA analysis of M6 yielded a value of  $\alpha = 0.58$ .

Because the DFA needs a minimum of 500 data points for the autocorrelation analysis of M6 the monthly mode of M6 had to be applied. To eliminate seasonal influences, we subtracted the seasonal mean value from the data and divided by the seasonal standard deviation. This yields a normalized record without seasonal effects that is appropriate for the DFA (Lennartz and Bunde, 2009). The result of  $\alpha = 0.58$  corresponds to other values for temperature series (Rybski and Bunde, 2009) and demonstrates that red noise as a background for M6 is not adequate. Therefore, one has to ascertain that the random records of the Monte-Carlo method simulating the background noise have the appropriate  $\alpha$  values. For this purpose we generated surrogate records with the Hurst exponents  $\alpha = 0.9$  for SPA and  $\alpha = 0.58$  for M6 by using a standard method (Turcotte, 1997).

The DFT without zero padding was applied for the reconstruction of M6 (Eqs. 1, 2). Here, we chose the basic method of selecting specific frequencies for the reverse transformation (Eq. 2) resulting directly in the reconstruction without any further optimization procedures. We find empirically that choosing among the first 8 frequencies of the DFT (which corresponds to all periods not shorter than 30 yr) the 6 frequencies with the strongest power densities yields an excellent reconstruction of M6. No other frequencies were applied.

#### 4 DFT and wavelet analysis

The left panel of Fig. 3 depicts the power densities of the DFT for M6 with padded zeros together with the 90 % and 95 % curves of confidence yielded by the Monte Carlo simulations. The right panel shows the same for SPA. Figure 4 shows the wavelet spectrum for the interpolated stalagmite record SPA. For M6 a wavelet analysis is meaningless

because of the shortness of the time series. Four of our six selected frequencies in M6 have a confidence level over 95 % and only one over 99 %. A rather good agreement of the frequency peaks between M6 and SPA exists for the periods of (roughly) 250, 80, 65, and 35 yr. A conspicuous disagreement is found for the peak with the period of 100 yr which is very strong in SPA and nearly lacks in M6.

We note that the 250 yr peak in Fig. 3 left results from only about one 250 yr period, which covers the entire record length. The question thus, if there is in fact a 250 yr periodicity, can only be decided by longer records. Fortunately the SPA record covers about 2000 yr. Its strong peak at 235 yr (Fig. 3 right) shows that a periodicity of this length is real. The wavelet diagram shows that this cycle has been the dominant one since about 1100 AD (see Fig. 4).

The wavelet analysis (Fig. 4) shows that historically a 125 yr cycle was dominating the earth temperature. During the many decades this cycle has weakened and the strength shifted to the subharmonic (see discussion) of 250 yr, which is now the dominant periodicity. In addition, the 4 lowest frequencies in Fig. 3 (right) show rather precisely the spectral pattern of the generation of the subharmonics (1, 0.5, 0.75, 1.25, which correspond to the periods 250, 500, 333, 200 yr). Such subharmonic generation is characteristic of systems with intrinsic dynamics (Feigenbaum, 1978, 1983).

## 5 Empirical reconstruction of the mean record M6

Our empirical reconstruction of M6 (hereafter RM6) with  $N = 254$  data points is based on the DFT without zero padding (Eq. 1). For the inverse transformation (Eq. 2) we selected empirically 6 periods (frequencies  $> 0$ ) obeying the conditions that they are longer than 30 yr and yield the strongest power densities among the first 8 DFT-frequencies  $i/N$ ,  $i = \{1, \dots, 8\}$ . As a result, the reconstruction is identical with the

## Multi-periodic climate dynamics

H.-J. Lüdecke et al.

Title Page

Abstract

Introduction

Conclusions

References

Tables

Figures

◀

▶

◀

▶

Back

Close

Full Screen / Esc

Printer-friendly Version

Interactive Discussion



restricted reverse transformation

$$f_k = \sum_j F_j W_N^{kj} \quad j = 0, 1, 3, 4, 5, 6, 7 \quad (3)$$

$$\text{RM6}(t) = \sum_j a_j \cos(2\pi jt/N) + b_j \sin(2\pi jt/N) \quad j = 0, 1, 3, 4, 5, 6, 7 \quad (4)$$

5 The parameter of Eq. (4) are given in Table 1.

Figure 5 depicts the comparison of the reconstruction RM6 and the record M6 after being boxcar-smoothed over 15 yr (hereafter SM6).

## 6 Confidence level of the reconstruction

10 The Pearson correlation of the smoothed record SM6 with the reconstruction RM6 (black and red curves in Fig. 5) has a value of  $r = 0.961$ . In order to ascertain the statistical confidence level of this accordance, we assumed a null hypothesis and evaluated it by Monte Carlo simulations based on random surrogate records of the same length and the same Hurst exponent ( $\alpha = 0.58$ ) as M6 generated by a standard method (Turcotte, 1997) (the surrogate records hereafter SU, and the boxcar-smoothed SU over 15 yr hereafter SSU). As the null hypothesis we assumed that the accordance of the reconstruction RM6 with SM6 is caused by chance. We applied 10 000 surrogate records 15 SU. Each of the record was analyzed following the same procedure as for M6. Next, for each surrogate SU the reconstruction was generated that used – again following the procedure as for M6 – 6 frequencies with the strongest power densities among the first 20 8 frequencies of the DFT without zero padding. Finally, the Pearson correlation of this reconstruction with SSU was evaluated. As a result, among 10 000 SU we found one surrogate record with the maximal  $r = 0.960$ , 9 records with  $r \geq 0.95$  and 53 records with  $r \geq 0.94$ . Therefore, the null hypothesis could be rejected with a confidence level of  $> 99.9\%$ .

## 7 Discussion

The temperature records from 6 Central European stations show remarkable agreement, justifying their averaging to produce a “Central European temperature record” M6. The characteristic of these records, namely the pronounced minimum around 1880 is equally found in Antarctic ice core temperature data, which are also overall in agreement with M6, revealing this 1880 minimum as a global phenomenon.

The Fourier transform of M6 yields pronounced spectral peaks, indicating dynamics by periodicity. Indeed, the inverse transform of the spectrum, in which nothing but the 6 strongest frequency components (with periods  $> 30$  yr) are retained, yields excellent agreement with the measurement M6. A temperature record obtained from a Central European stalagmite is also Fourier-analyzed, and shows, for comparison, similar periodicities. The cause of the periodicities is unknown. We would think that they constitute intrinsic system dynamics as it is generally found for dissipative systems with energy input (here the earth dissipating the radiative energy provided by the sun), such dynamics being the physics behind all terrestrial weather dynamics (e.g. trade winds or El Niño). This interpretation as intrinsic system dynamics is supported by the wavelet analysis of the stalagmite data. The latter shows a drift over 1600 yr of peak intensity from the 128 yr period to the 256 yr period. Such a shifting of energy from a fundamental to a subharmonic frequency component is characteristic of the Feigenbaum universal scenario of transition to chaos by a cascade of subharmonics, for nonlinear, driven, dissipative systems (Feigenbaum, 1978, 1983). Whereas harmonic generation is just an expression of nonlinearity, subharmonic generation is peculiar to the Feigenbaum scenario, since it requires, different from harmonic generation, a particular phase-matching mechanism. The 4 lowest frequency lines of Fig. 3 (right) give additionally evidence of the climate oscillations as intrinsic dynamics. They show the pattern characteristic of generation of two subharmonics which corresponds rather convincingly to the Feigenbaum transition to Chaos. Such a transition requires the continuous, monotonic change of a “control parameter”. The world temperature which is recently found to drop

CPD

8, 4493–4511, 2012

### Multi-periodic climate dynamics

H.-J. Lüdecke et al.

Title Page

Abstract

Introduction

Conclusions

References

Tables

Figures

◀

▶

◀

▶

Back

Close

Full Screen / Esc

Printer-friendly Version

Interactive Discussion



continuously over the last 2000 yr (Esper et al., 2012), may well have the role of “control parameter” here.

The excellent agreement of the reconstruction of the temperature history, using only the 6 strongest frequency components of the spectrum, with M6 would leave, together with the agreement of temperatures in the Northern and Southern Hemisphere, no room for any influences of CO<sub>2</sub> or other anthropogenic emissions or effects on the Earth’s climate.

We note that the prediction of a rather substantial temperature drop of the Earth over the next decades (dashed blue line in Fig. 5) results essentially from the ~ 64 yr periodicity, of which 4 cycles are clearly visible in Fig. 5; and which, consequently, can be expected to reliably repeat in the future.

*Acknowledgements.* We thank Régine Larrieu (météo france, Toulouse) for kindly allocating the Paris time series for our studies. We thank Luboš Motl for his technical information about the Prague record.

## References

Auer, I., Böhm, R., Jurkovic, A., Lipa, W., Orlik, A., Potzmann, R., Schöner, W., Ungersböck, M., Matulla, C., Briffa, K., Jones, P., Efthymiadis, D., Brunetti, M., Nanni, T., Maugeri, M., Mercalli, L., Mestre, O., Moisselin, J.-M., Begert, M., Müller-Westermeier, G., Kveton, V., Bochnicek, O., Stastny, P., Lapin, M., Szalai, S., Szentimrey, T., Cegnar, T., Dolinar, M., Gajik-Capka, M., Zaninovic, K., Majstorovic, Z., and Nieplova, E.: HISTALP – historical instrumental climatological surface time series of the Greater Alpine Region, *Int. J. Climatol.*, 27, 17–46, 2007. 4494, 4496

Czech Hydrometeorological Institute, 143 06 Praha 4 Czech Republic, available at: <http://zmeny-klima.ic.cz/klementinum-data/> (last access: August 2012), 2012. 4494, 4496

Climatic Research Unit (CRU), University of East Anglia (UK), available at: [www.cru.uea.ac.uk/cru/data/temperature/station-data/](http://www.cru.uea.ac.uk/cru/data/temperature/station-data/) (last access: August 2012), 2012. 4494, 4496

Deutscher Wetterdienst (DWD), Frankfurter Straße 135, 63067 Offenbach (Germany), available at: [www.dwd.de](http://www.dwd.de) (last access: August 2012), 2012. 4494, 4496

## Multi-periodic climate dynamics

H.-J. Lüdecke et al.

Title Page

Abstract

Introduction

Conclusions

References

Tables

Figures



Back

Close

Full Screen / Esc

Printer-friendly Version

Interactive Discussion



**Multi-periodic  
climate dynamics**

H.-J. Lüdecke et al.

Title Page

Abstract

Introduction

Conclusions

References

Tables

Figures

◀

▶

◀

▶

Back

Close

Full Screen / Esc

Printer-friendly Version

Interactive Discussion



- Esper, J., Frank, D. C., Timonen, M., Zorita, E., Wilson, R. J. S., Luterbacher, J., Holzkämper, S., Fischer, N., Wagner, S., Nievergelt, D., Verstege, A., and Büntgen, U.: Orbital forcing of tree-ring data, *Nat. Clim. Change*, in press, doi:10.1038/NCLIMATE1589, 2012. 4502
- 5 Feigenbaum, M. J.: Quantitative universality for a class of nonlinear transformations, *J. Stat. Phys.*, 19, 25–51, 1978. 4499, 4501
- Feigenbaum, M. J.: Universal behavior in nonlinear systems, *Physica D*, 7, 16–39, 1983. 4499, 4501
- Ghil, L., Allen, M. R., Dettinger, M. D., Ide, K., Kondrashov, D., Mann, M. E., Robertson, A. W., Saunders, A., Tian, Y., Varadi, F., and Yiou, P.: Advanced spectral methods for climatic time series, *Rev. Geophys.*, 40, 1–41, 2002. 4496
- 10 Graf, W., Oerter, H., Reinwarth, O., Stichler, W., Wilhelms, F., Miller, H., and Mulvaney, R.: Stable-isotope records from Dronning Maud Land, Antarctica, *Ann. Glaciol.*, 35, 195–201, 2002. 4495, 4496
- Horne, J. H. and Baliunas, S. L.: A prescription for period analysis of unevenly sampled time series, *The Astrophysical Journal*, 302, 757–763, 1986. 4497
- Kantelhardt, J. W.: Fluktuationen in komplexen Systemen, Habilitationsschrift, Universität Gießen, Germany, 19 June, available at: [www.physik.uni-halle.de/Fachgruppen/kantel/habil.pdf](http://www.physik.uni-halle.de/Fachgruppen/kantel/habil.pdf) (last access: August 2012), 2004. 4497
- Lennartz, S. and Bunde, A.: Trend evaluation in records with long-term memory: application to global warming, *Geophys. Res. Lett.*, 36, L16706, doi:10.1029/2009GL039516, 2009. 4497, 4498
- 20 Lennartz, S. and Bunde, A.: Distribution of natural trends in long-term correlated records: a scaling approach, *Phys. Rev.*, E84, 021129, doi:10.1103/PhysRevE.84.021129, 2011. 4497
- Lüdecke, H.-J.: Long-term instrumental and reconstructed temperature records contradict anthropogenic global warming, *Energy & Environment*, 22, 723–745, 2011. 4498
- 25 Mangini, A., Spötl, C., and Verdes, P.: Reconstruction of temperature in the Central Alps during the past 2000 years from a <sup>18</sup>O stalagmite record, *Earth Planet. Sc. Lett.*, 235, 741–751, 2005. 4495, 4496
- Météo France: 42 Av. Gaspard Coriolis, 31057 Toulouse Cedex (France), 2012. 4494, 4496
- 30 Rybski, D. and Bunde, A.: On the detection of trends in long-term correlated records, *Physica A*, 388, 1687–1695, 2009. 4498
- Schulz, M. and Mudelsee, M.: REDFIT: estimating red-noise spectra directly from unevenly spaced paleoclimatic time series, *Comput. Geosci.*, 28, 421–426, 2002. 4497

- Torrence, C. and Compo, P.: A practical guide to wavelet analysis, B. Am. Meteorol. Soc., 79, 61–78, 1998. 4510
- Torrence, C. and Compo, P.: Wavelet software, available at: <http://atoc.colorado.edu/research/wavelets/> (last access: August 2012), 2012. 4510
- 5 Turcotte, D. L.: Fractals and Chaos in Geology and Geophysics, 2nd Edition., Cambridge University Press, Cambridge, 1997. 4498, 4500

## Multi-periodic climate dynamics

H.-J. Lüdecke et al.

Title Page

Abstract

Introduction

Conclusions

References

Tables

Figures



Back

Close

Full Screen / Esc

Printer-friendly Version

Interactive Discussion



## Multi-periodic climate dynamics

H.-J. Lüdecke et al.

**Table 1.** Frequencies, periods, and the coefficients  $a_j$  and  $b_j$  of the reconstruction RM6 due to Eqs. (1), (3), and (4) ( $N = 254$ ).

$j$	$j/N$ ( $\text{yr}^{-1}$ )	Period (yr)	$a_j$	$b_j$
0	0	–	0	0
1	0.00394	254	0.68598	–0.12989
2	0.00787	127	–	–
3	0.01181	85	0.19492	–0.14677
4	0.01575	64	0.17465	–0.22377
5	0.01968	51	0.14730	–0.10810
6	0.02362	42	–0.02510	–0.12095
7	0.02756	36	0.12691	0.01276
8	0.03150	32	–	–

Title Page

Abstract

Introduction

Conclusions

References

Tables

Figures

◀

▶

◀

▶

Back

Close

Full Screen / Esc

Printer-friendly Version

Interactive Discussion



**Multi-periodic  
climate dynamics**

H.-J. Lüdecke et al.

Title Page

Abstract

Introduction

Conclusions

References

Tables

Figures

◀

▶

◀

▶

Back

Close

Full Screen / Esc

Printer-friendly Version

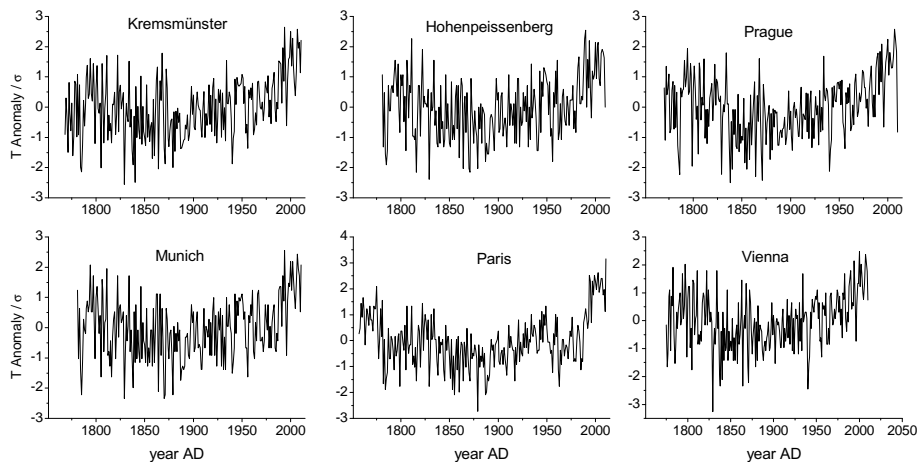
Interactive Discussion

**Table A1.** Abbreviations of the time series in this paper.

IC	Ice core record as yearly $\delta^{18}\text{O}$ values.
M6	Mean of 6 instrumental records in Central Europe (both monthly and yearly).
RM6	Reconstruction of M6.
SPA	Stalagmite time series as yearly temperatures yielded by interpolation.
SM6	M6 smoothed over 15 yr (boxcar).
SU	Surrogate records with Hurst exponents $\alpha = 0.58 \pm 0.3$ .
SSU	Smoothed SU over 15 yr (boxcar).

**Multi-periodic  
climate dynamics**

H.-J. Lüdecke et al.

**Fig. 1.** Long-term temperature records from 6 Central European stations.

Title Page

Abstract

Introduction

Conclusions

References

Tables

Figures

◀

▶

◀

▶

Back

Close

Full Screen / Esc

Printer-friendly Version

Interactive Discussion



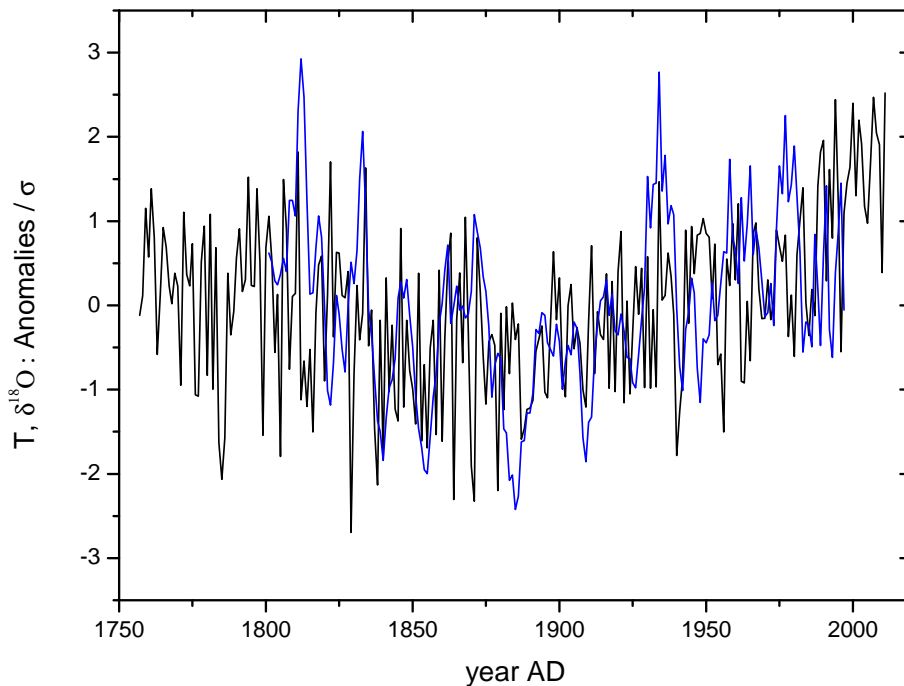


**Fig. 2.** (color online): Instrumental temperature averaged record M6 (black) together with the Antarctic ice core record IC (blue), each as an anomaly divided by the standard deviation.

**Multi-periodic climate dynamics**

H.-J. Lüdecke et al.

Title Page

Abstract Introduction

Conclusions References

Tables Figures

◀ ▶

◀ ▶

Back Close

Full Screen / Esc

Printer-friendly Version

Interactive Discussion



Multi-periodic  
climate dynamics

H.-J. Lüdecke et al.

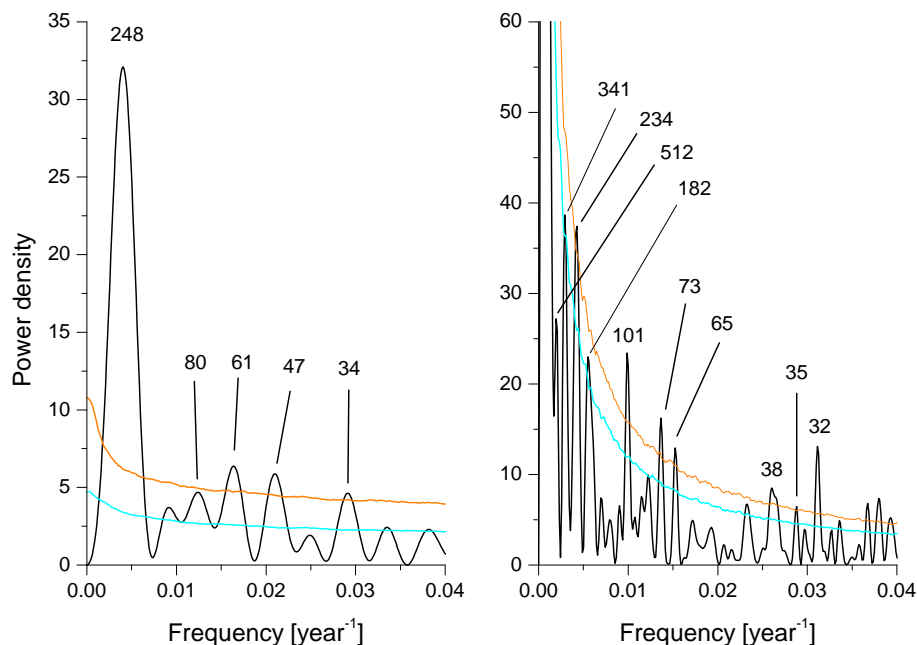


**Fig. 3.** (color online) Left panel: DFT of M6 (average from 6 Central European instrumental time series). Right panel: same for SPA, interpolated time series of a stalagmite from the Austrian Alps for the period 500–1935 AD. In both DFT analyses the records were padded with zeros. The upper confidence curve (brown) is for 95 %, the lower (cyan) for 90 % against background noise, each of those established by 10 000 Monte Carlo runs. The most relevant peaks are indicated by their period length.

Title Page

Abstract

Introduction

Conclusions

References

Tables

Figures

◀

▶

◀

▶

Back

Close

Full Screen / Esc

Printer-friendly Version

Interactive Discussion



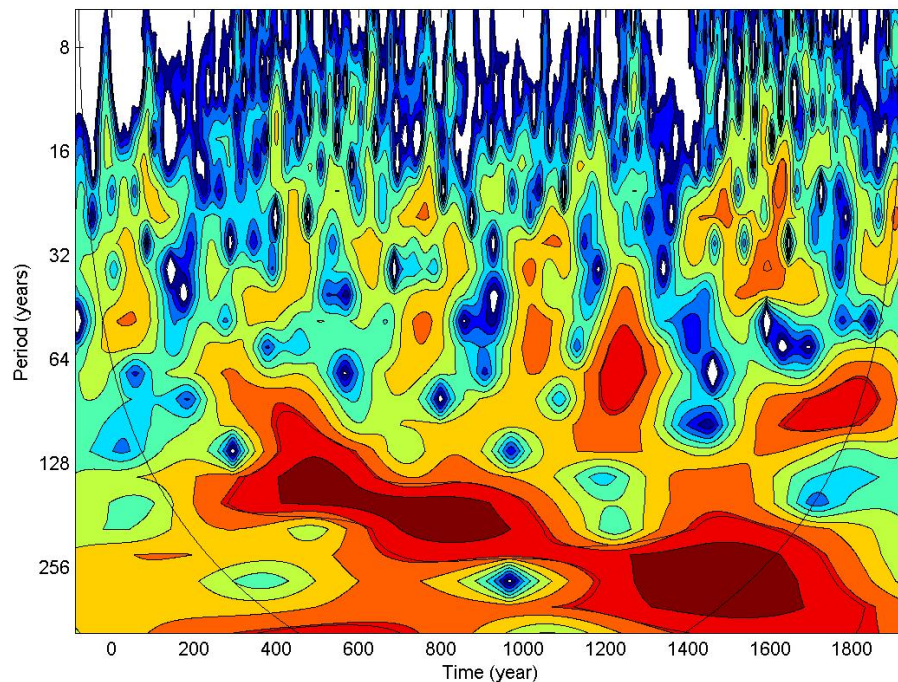


**Fig. 4.** (color online) Wavelet (Morlet) spectrum (Torrence and Compo, 1998), (Torrence and Compo, 2012) of the interpolated SPA record for the period 90 BC until 1935 AD. The solid black line from the left to the right top of the figure is the cone of influence (below the coi the results are not significant). The spectrum shows that the power density between the period of 128 and 256 yr is moving with increasing time to lower frequencies. This area is only badly resolved in M6 (see Fig. 3, left panel).

**Multi-periodic climate dynamics**

H.-J. Lüdecke et al.

Title Page

Abstract Introduction

Conclusions References

Tables Figures

◀ ▶

◀ ▶

Back Close

Full Screen / Esc

Printer-friendly Version

Interactive Discussion



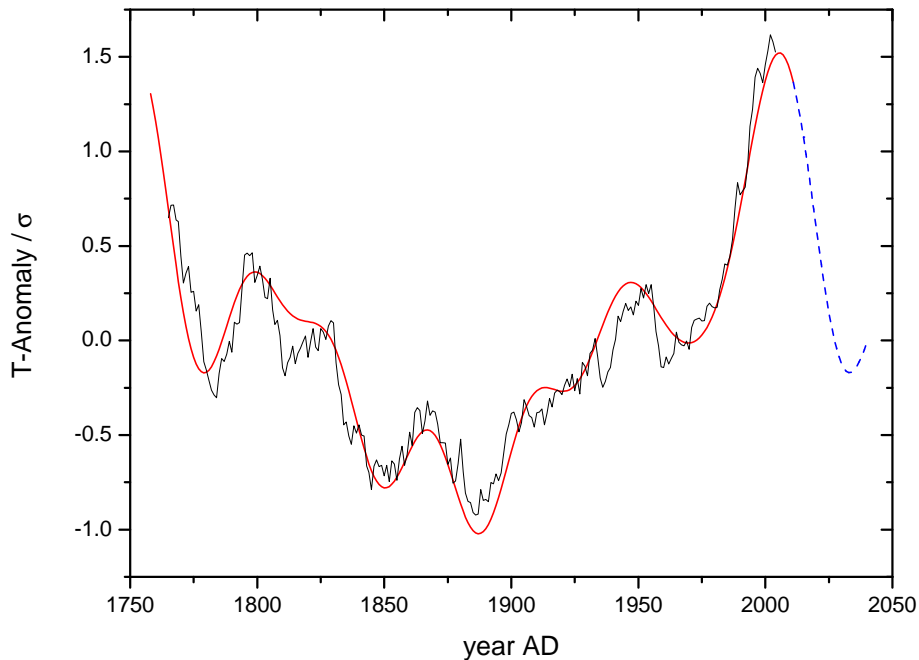


**Fig. 5.** (color online) 15 yr running average record SM6 (black); reconstruction RM6 according to Eqs. (1), (3), (4) (red); continuation of the reconstruction for the next three decades (dashed, blue) corresponds to the beginning of the reconstruction due to the properties of the Fourier transformation.

**Multi-periodic climate dynamics**

H.-J. Lüdecke et al.

Title Page

Abstract

Introduction

Conclusions

References

Tables

Figures

◀

▶

◀

▶

Back

Close

Full Screen / Esc

Printer-friendly Version

Interactive Discussion

